Available online at www.sciencedirect.com
ScienceDirect
Journal of Molecular Catalysis A: Chemical 267 (2007) 129–136
JOURNAL OF MOLECULAR CATALYSIS A: CHEMICAL
www.elsevier.com/locate/molcata

Reactivity of zirconium and titanium alkoxides bidentade complexes on ethylene polymerization

Nara R. de S. Basso [a,*], Paula P. Greco [a], Carlos L.P. Carone [b], Paolo R. Livotto [b], Lílian M.T. Simplício [c], Zênis N. da Rocha [c], Griselda B. Galland [b], João H.Z. dos Santos [b]

[a] *Laboratório de Organometálicos e Resinas, Faculdade de Química, PUCRS, Av. Ipiranga 6681, Porto Alegre 90619-900, Brazil*
[b] *Laboratório Catálise Ziegler-Natta, Instituto de Química, UFRGS, Av. Bento Gonçalves 9500, Porto Alegre 91570-970, Brazil*
[c] *Instituto de Química da Universidade Federal da Bahia, Campus de Ondina, Salvador 40170-290, Brazil*

Received 10 October 2006; received in revised form 13 November 2006; accepted 14 November 2006
Available online 21 November 2006

Abstract

The catalyst activity of zirconium and titanium complexes bearing bidentade ligands was evaluated in ethylene polymerization at different experimental conditions with methylaluminoxane (MAO) as the cocatalyst. The best activity was achieved for dichlorobis(3-hydroxy-2-methyl-4-pyrone)zirconium(IV) at Al/Zr = 2500 at 60 °C. Conversely, dichlorobis(3-hydroxy-2-methyl-4-pyrone)titanium(IV) exhibited a higher catalyst activity at lower Al/Ti ratio and temperature. According to ^{1}H NMR analysis, two stereoisomers are present for the zirconium complex. Electrochemical analyses evidenced a higher stability in the reduction of Zr(IV) in comparison to the analogous Ti(IV) complex. The cyclic voltammogram of the Ti complex in the presence of MAO and ethylene shows a potential shift to lower values, suggesting the formation of the Ti cationic species, which might be stabilized by ClMAO$^-$. For the Zr complex in the presence of MAO, stabilization of the active species takes place only in the presence of an ethylene atmosphere.

Keywords: Titanium alkoxide; Zirconium alkoxide; Polyethylene; Polymerization; Non-metallocene catalyst

1. Introduction

Much research has been conducted on olefin polymerization catalysis aimed at developing new catalyst systems capable of producing new materials, as well as more economic and versatile processes. New non-metallocene complexes bearing ancillary ligands such as amido, alkoxo, tris(pyrazolyl)borate, diketimine and related polydentate ligands have appeared as a new trend in this field of research [1–6]. Sobota and co-workers have synthesized and evaluated the catalytic activity of the complex dichlorobis(3-hydroxy-2-methyl-4-pyrone)titanium(IV) in the ethylene polymerization, suggesting that this ligand represents a good alternative for the cyclopentadienyl ring [7]. Recently, we have synthesized the analogous zirconium complex, dichlorobis(3-hydroxy-2-methyl-4-pyrone)zirconium(IV), and the catalytic activity on ethylene polymerization of both complexes has been investigated in homogeneous and heterogeneous conditions [8,9].

The molecular structure analysis of these complexes and the investigation of the chemical behavior of the intermediate species can elucidate aspects related to reactivity and selectivity in polymerization reactions. A few studies devoted to such compounds are found in the literature. Crystallographic and electrochemical analysis of the dichlorobis(3-hydroxy-2-methyl-4-pyrone)titanium(IV) complex was conducted by Sobota [7], however the analogous zirconium complex was not investigated in his work. In the present paper, we reported the behavior of dichlorobis(3-hydroxy-2-methyl-4-pyrone)titanium(IV) and dichlorobis(3-hydroxy-2-methyl-4-pyrone)zirconium(IV) in ethylene polymerization with MAO as the cocatalyst. The complexes' reactivity and stability were also monitored by cyclic voltammetry.

* Corresponding author. Tel.: +55 51 3320 3549; fax: +55 51 3320 3612.
E-mail address: nrbass@pucrs.br (N.R.d.S. Basso).

1381-1169/$ – see front matter © 2006 Elsevier B.V. All rights reserved.
doi:10.1016/j.molcata.2006.11.027

2. Experimental

2.1. General procedures

All experiments were performed under an Ar atmosphere using Schlenk-type glassware. Tetrahydrofuran (THF), hexane and toluene were distilled from sodium and benzophenone. Dichloromethane was dried by refluxing over phosphorus pentoxide. Acetonitrile (Merck), spectroscopic grade used as the solvent in cyclic voltammetry experiments, was dried over molecular sieves and distilled. The ligand 3-hydroxy-2-methyl-4-pyrone (Aldrich), $TiCl_4$ (Merck) and $ZrCl_4$ (Merck) were used without further purification. MAO (Witco, 5.21% (w/w) Al in toluene solution was employed as received.

2.2. Cyclic voltammetry

The cyclic voltammetry (CV), differential pulse voltammetry (DPV) and constant potential electrolysis (coulometry) measurements were taken with a potentiostat/galvanostat (PARC, model 273). All experiments were carried out using a conventional three electrode cell. Glassy carbon was used as a working electrode for CV and platinum gauze for coulometry. An Ag/AgCl electrode was used as the reference electrode and a platinum wire as the auxiliary electrode. Electrochemical data were obtained using 0.1 mol L^{-1} solutions of tetrabutylammonium tetrafluoroborate in acetonitrile as the supporting electrolyte. In the cyclic voltammograms, neither anodic nor cathodic peaks were observed in the absence of titanium or zirconium complexes in the potential range studied. All solutions were deaerated by bubbling with high purity argon. The cocatalyst solutions were prepared with different Al/Zr molar ratios between 0 and 10 and the cyclic voltammograms were recorded with a scan rate of 100 mV s^{-1}. Ferrocene (+0.50 V versus Ag/AgCl), was employed as an internal standard in acetonitrile solution.

The spectroelectrochemical measurements were carried out using a gold mini-grid working electrode, Ag/AgCl as a reference and platinum wire as an auxiliary electrode and quartz cell with a 0.030 cm optical path. The electronic absorption spectra were recorded using Hewlett Packard Modeles 8453. Successive spectra were recorded during the redox process of the complexes.

2.3. Theoretical calculations

The energy of all calculated species was obtained by full geometry optimization without any constraint. The calculations were performed with the Gaussian 98 Program [10], at a HF/B3LYP [11,12] level of theory, using a Dunning-Huzinaga DZ95 [13] basis set complemented with polarization functions for the non-metal atoms and a DZ valence basis set plus an effective core potential [14–16] for the zirconium.

2.4. Polymerization reactions

Ethylene polymerizations were performed in 0.3 L of toluene in a 1.0 L Pyrex glass reactor connected to a constant temperature circulator, equipped with a mechanical stirrer, and inlets for argon and the monomer. MAO was used as the cocatalyst in Al/M molar ratios between 250 and 2500. For each experiment, 1×10^{-5} or 1×10^{-6} mol of catalyst was suspended in toluene or hexane and transferred into the reactor under argon. The polymerizations were performed at 1.6 atm of ethylene at different temperatures, for 60 min. The reagents were introduced into the reactor in the following order: solvent, cocatalyst, ethylene and catalyst. Acidified (HCl) ethanol was used to quench the process, and reaction products were separated by filtration, washed with distilled water, and finally dried under reduced pressure at room temperature.

2.5. Polymer characterization

The melting points (T_m) and crystallinities (χ_c) of the polymers were determined by using a differential scanning calorimeter (Perkin-Elmer, DSC-4), at a heating and cooling rate of 10 °C min^{-1} in the temperature range of 30–160 °C. The heating cycle was performed twice, but only the results of the second scan are reported. Average molecular weight and molecular weight distributions were investigated with a Water high-temperature GPC instrument, CV plus system, Model 150C, equipped with optic differential refractometer and three Styragel HT type columns (HT3, HT4 and HT6) with an exclusion limit 1×10^7 for polystyrene. 1,2,4-Trichlorobenzene was used as the solvent, at a flow rate of 1 L min^{-1}. The analyses were performed at 140 °C. The columns were calibrated with standard narrow molar mass distribution polystyrenes and then universally with linear low density polyethylenes and polypropylenes.

2.6. Isomers characterization

The ^1H NMR spectra of the zirconium complex were prepared in DMSO-d_6 and recorded on a Varian Inova 300 spectrometer operating at 300 MHz.

3. Results and discussion

3.1. Polymerization

The dichlorobis(3-hydroxy-2methyl-4-pyrone)titanium(IV) (**1**) and dichlorobis(3-hydroxy-2-methyl-4-pyrone)zirconium (IV) (**2**) complexes (Scheme 1) were synthesized from the complexation of the ligand 3-hydroxy-2-methyl-4-pyrone to the respective metal salt, MCl_4 (M = Ti or Zr) in THF [7,8].

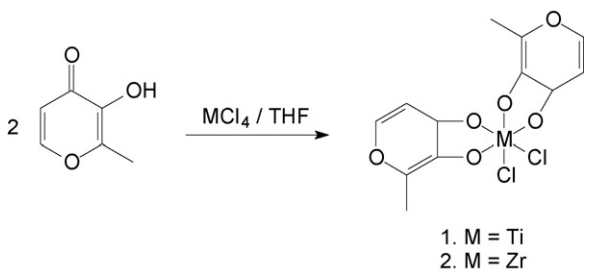

Scheme 1.

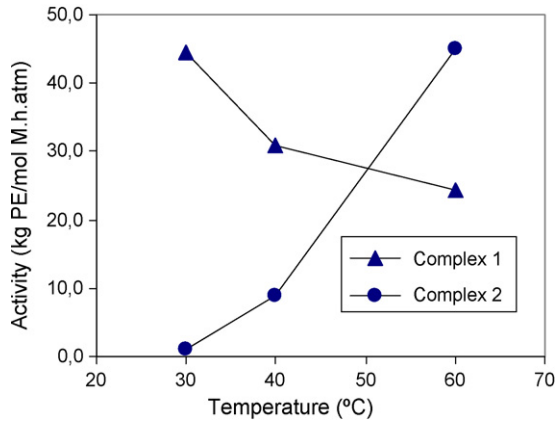

Fig. 1. Influence of polymerization temperature on the catalyst activity.

Catalytic activities of the complexes **1** and **2** were evaluated in homogeneous ethylene homopolymerization in different experimental conditions. Fig. 1 shows the influence of polymerization temperature on the catalyst activity.

According to Fig. 1, catalyst activity was shown to depend on the complex's metal center. In the evaluated range, increasing the temperature from 30 to 60 °C decreases catalyst activity in the case of the titanium complex, but increases it in the case of zirconium. This behavior is similar to that already reported for titanocene and zirconocene complexes, in which a reduction in catalyst activity in the case of titanocene is probably due to thermal lability of such complexes [17].

Fig. 2 shows the influence of Al/Ti ratio for complex **1** at 60 °C.

According to Fig. 2, in the evaluated range, increasing Al/Ti ratio results in a reduction in catalyst activity. Similar behavior has already been reported for zirconocene catalysts and this catalyst activity reduction was attributed to the equilibrium shift in the direction of the ionic pair association between the cationic species and MAO [18]. Nevertheless, in the present case, one cannot neglect the possibility of overreduction of the Ti center, or inactive species in α-olefin polimerization, due to traces of trimethylaluminum, which might be present in commercial MAO solution.

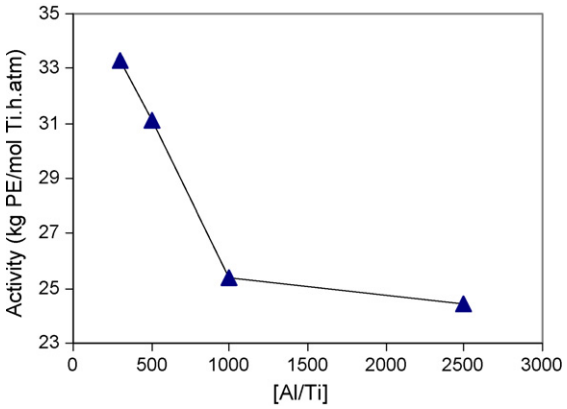

Fig. 2. Influence of the Al/Ti molar ratio on the catalyst activity of complex **1**.

Table 1
Catalytic activity of zirconium and titanium complexes

Entry	Catalyst	Al/M	T (°C)	Activity[a]	T_m (°C)	χ_c (%)
1	**1**	2500	30	44.4	132	39
2	**1**	2500	40	30.9	133	25
3	**1**	2500	60	24.4	133	36
4	**2**	2500	30	1.1	130	10
5	**2**	2500	40	8.8	133	61
6	**2**	2500	60	45.0	135	67
7	**1**	1000	60	25.4	133	31
8	**1**	500	60	31.1	130	38
9	**1**	300	60	33.3	132	13
10	**2**	1000	60	14.4	128	44
11[b]	**1**	1000	40	66.0	132	10
12[b]	**1**	1000	60	54.2	133	31
13[b]	**1**	250	40	12.9	132	47
14[b]	**2**	2500	60	180.0	135	41

Solvent: toluene; ethylene: 1.6 atm; time: 60 min; [M]: 10^{-6} mol; χ_c: crystallinity.
[a] Expressed in kg PE/(mol M h atm).
[b] [M] = 10^{-5} mol.

The set of evaluated polymerization conditions as well as polymer melting temperature and crystallinity are gathered in Table 1.

According to Table 1, in terms of Al/M ratio, an opposite trend was observed in the case of complex **2**: An increasing of Al/Zr ratio affords better catalyst activity, as shown by entries 6 and 10. Resulting polyethylenes produced by both complexes have the melting temperatures typical of high density polyethylenes. Weight average molecular weights and molecular weight distributions are 500.000 g/mol and 3.9 and 430.000 and 2.8 for the polyethylenes obtained with the titanocene catalyst (entries 11 and 12, respectively) and 161.800 g/mol and 1.9 for the zirconocene catalyst (entry 14).

3.2. Stereoisomers

Recrystallization of the zirconium complex results in white crystals in the shape of fine needles which became light yellow after a few weeks under argon atmosphere. NMR in DMSO-d_6 spectrum shows two main stereoisomers **A** and **B**, as shown in Fig. 3. Stereoisomer **A** shows the following chemical shifts: Ha, d, 8.48 ppm; Hb, d, 6.82 ppm and CH_3, s, 2.35 ppm and stereoisomer **B** shows Ha, d, 8.34 ppm, Hb, d, 6.72 ppm and CH_3, s, 2.28 ppm. The ratio of the isomers was determined by integrating the ^{1}H NMR signals, using three corresponding resonances for each isomer. Table 2 shows a study of spectra obtained from catalysts which were synthesized on different dates and with different DMSO-d_6 solution times. The obtained complex before recrystallization is composed mainly of 77% of isomer **A** and 23% of **B**. The recrystallization of the complex in hexane resulted in crystals of mainly isomer **B** (81.3%). A spectrum of the crystals kept 15 h in DMSO-d_6 showed 59.2% **A**. Three days later showed 66.4% of isomer **A** and a month later 73.7%, signaling interconversion of the two stereoisomers. This interconversion results mainly in isomer **A**, suggesting that this isomer is more stable than **B** in DMSO.

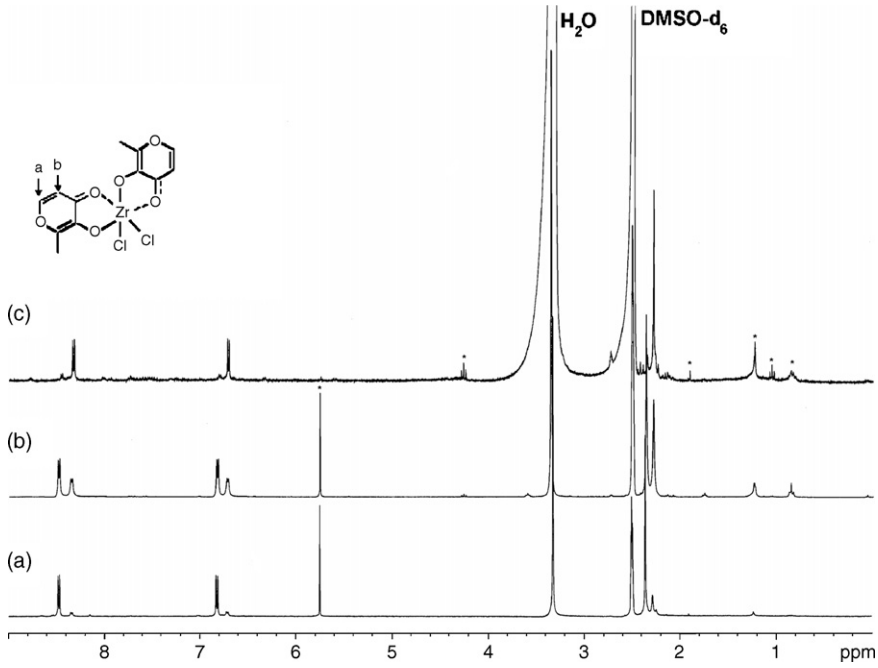

Fig. 3. Zirconium complex ^{1}H NMR: (a) synthesis 1 of the zirconium complex; (b) crystals in 15 h later in DMSO-d_6; (c) white crystals. (*) Impurity.

Complex **2** crystallizes in the shape of very fine needles that hinder a monocrystal separation suitable for X-ray monocrystal diffraction in order to elucidate stereoisomeric structure.

Theoretically, there are four possible isomers for the zirconium complex, as it is suggested in Scheme 2. *Trans* isomers polarity must be close to zero and the *cis* isomers polarity different than zero because the polarity vectors do not cancel each other. As the complex recrystallization was performed in hexane, this apolar solvent engenders the *trans* geometry. However, a polar solvent as DMSO, should lead to the *cis* geometry. The polarity shift from an apolar to a polar solvent favors the interconvention from *trans* to *cis* isomer.

A study of the energy of the stereoisomers by Density Functional Theory method showed that ***Cis* I** is 2.56 kcal/mol more stable than ***Cis* II**, which in turn is 0.86 kcal/mol more stable than ***Trans* II**. The latter is 6.50 kcal/mol more stable than ***Trans* I**. Considering the energy of these isomers, we suggest that isomer

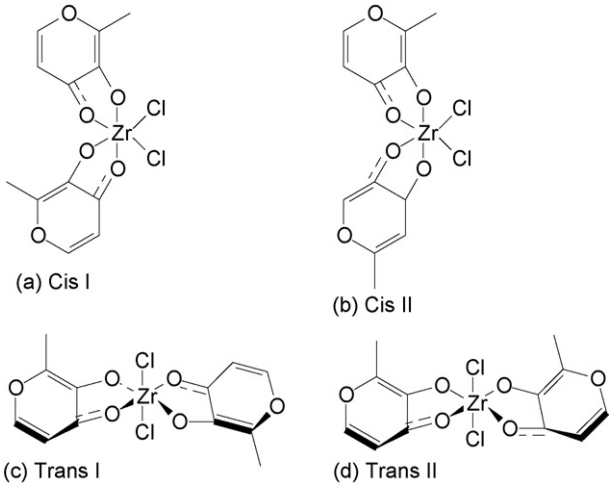

Scheme 2.

Table 2
Proportion of the **A** and **B** isomers calculated from ^{1}H NMR study

Samples	8.48 ppm (%)	8.34 ppm (%)	6.82 ppm (%)	6.72 ppm (%)	2.35 ppm (%)	2.28 ppm (%)	Isomer **A** (average) (%)	Isomer **B** (average) (%)
Synthesis 1	81.3	18.7	79.4	20.6	78.2	21.2	79.6	20.4
Synthesis 2	78.0	22.0	74.5	25.5	74.4	25.6	75.6	24.4
Synthesis 3	79.6	20.4	75.3	24.7	76.1	23.9	77.0	23.0
Synthesis 4	79.6	20.4	73.9	26.1	76.0	24.0	76.5	23.5
Crystals	19.2	80.8	19.2	80.8	17.7	82.3	18.7	81.3
Crystals after 15 h in DMSO	59.7	40.3	59.7	40.3	58.1	41.8	59.2	40.8
Crystals after 3 days in DMSO	67.3	32.7	67.0	33.0	64.9	35.1	66.4	33.6
Crystals after 1 month in DMSO	75.4	24.6	73.8	26.2	71.9	28.1	73.7	26.3

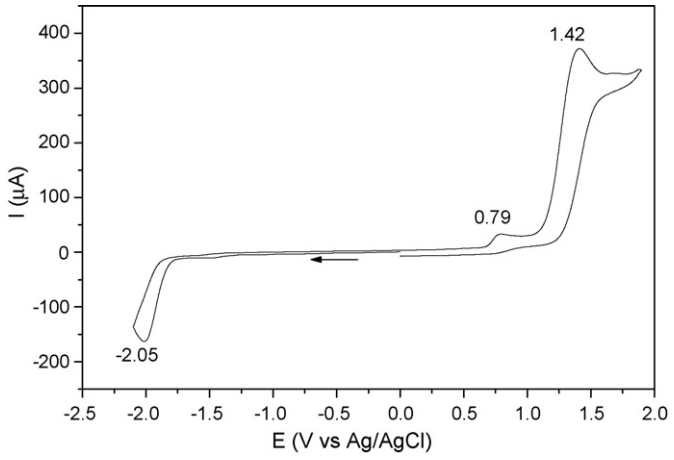

Fig. 4. Cyclic voltamogram of the ligand 3-hydroxy-2-methyl-4-pyrone (pyrone).

B is *trans* and **A** is *cis*, because they are more stable. Only *cis* isomers are capable of polymerizing ethylene [19].

The presence of a stereoisomer was not verified for the analogous titanium complex **1**, and its structure, proposed in the literature, is in accordance with the structure of ***Cis* I** isomer suggested for the zirconium complex in this paper.

3.3. Electrochemical analysis

The electrochemical behavior of the complexes **1** and **2** was investigated by cyclic voltammetry, differential pulse voltammetry and controlled potential electrolysis.

In the cyclic voltammogram of the pyrone organic ligand (Fig. 4), the peaks (or waves) indicate an oxidation process at +0.79 and +1.42 V and another one referring to a reduction process at −2.0 V, in accordance to the literature [2]. There is also a reduction peak of low intensity at −1.5 V. All peaks are independent of the sweep in the positive or negative direction potential.

Cathodic waves for the complexes **1** and **2** are observed in Fig. 5. The cathodic peaks at −0.48, −0.72, −1.52 and −1.9 V might be related to the reduction process on the metallic center for the titanium complex, $[TiCl_2(pyrone)_2]$, because electrochemical reduction does not occur on the ligand in this region. The first, second and last cathodic waves have their corresponding anodic currents at −0.4, −0.65 and −2.1 V, respectively, versus Ag/AgCl, with peak separations consistent with a one electron process.

The cyclic voltammogram of zirconium complex, $[ZrCl_2(pyrone)_2]$, run over a potential range of +0.4 to −2.2 V versus Ag/AgCl at a potential scan rate of $v = 100\,mV\,s^{-1}$ shows cathodic waves at −1.3 and −1.8 V. In the reverse potential sweep no corresponding anodic waves were observed (Fig. 5b). These peaks are assigned to the reduction of the metal center. The absence of an anodic wave was illustrated in cyclic voltammograms for runs in the potential range from +0.4 to −1.5 V versus Ag/AgCl at a potential scan rate $v = 50$–$800\,mV\,s^{-1}$. However, the profile of differential pulse voltammograms showed that

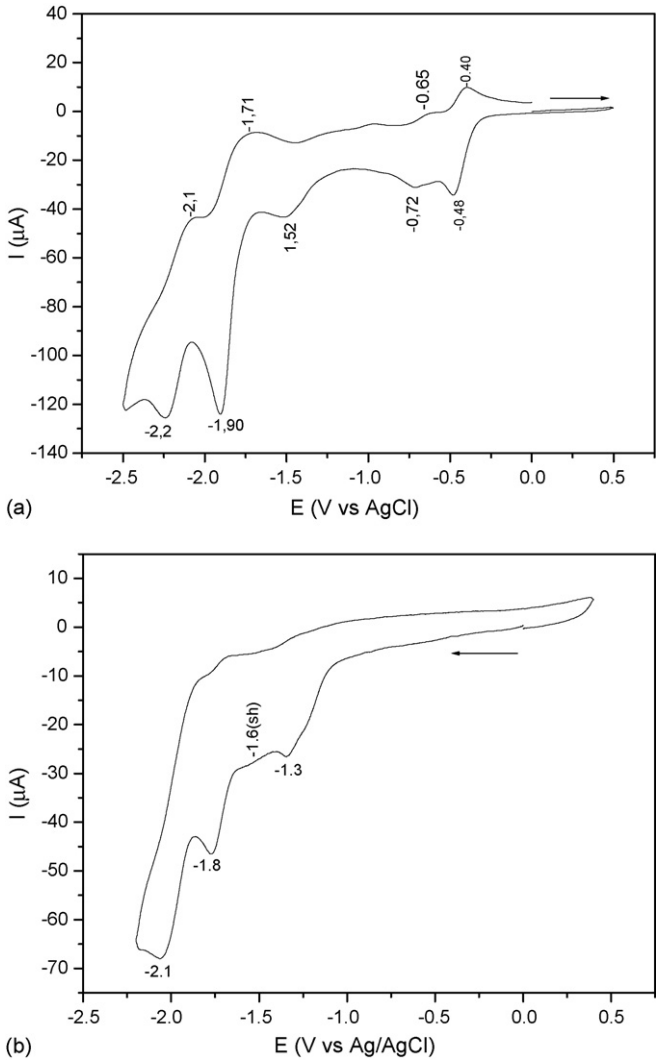

Fig. 5. Cyclic voltammogram of the $[TiCl_2(pyrone)_2]$ (a) and $[ZrCl_2(pyrone)_2]$ (b) complexes.

cathodic waves have corresponding anodic waves. These results are consistent with a reversible electrode process.

Differential pulse voltammograms for $[ZrCl_2(pyrone)_2]$ with a cathodic scan shows cathodic waves (−1.2 (shifted if compared with VC), −1.6 and −2.1 V) were observed at $72.72\,mV\,s^{-1}$. Nevertheless, by decreasing the scan rate, another peak was detected at −1.8 V (Fig. 6a). In the anodic scan, additional anodic waves assigned to the metal center and to coordinated pyrone were observed. A wave at −1.9 V was assigned the oxidation of the pyrone ligand (Fig. 6b). An anodic wave at −1.4 V was detected, but further investigation will be done to assign this peak. The results are consistent with a reversible electrode process followed by a chemical reaction. Likely, labilization of the pyrone ligand has taken place. Controlled potential electrolysis results confirmed this proposition.

The cathodic peak at −1.9V (Fig. 5a) in the titanium complex can be considered a result of the spontaneous conversion of the initial complex into other species through ligand release (Eq. (3)).

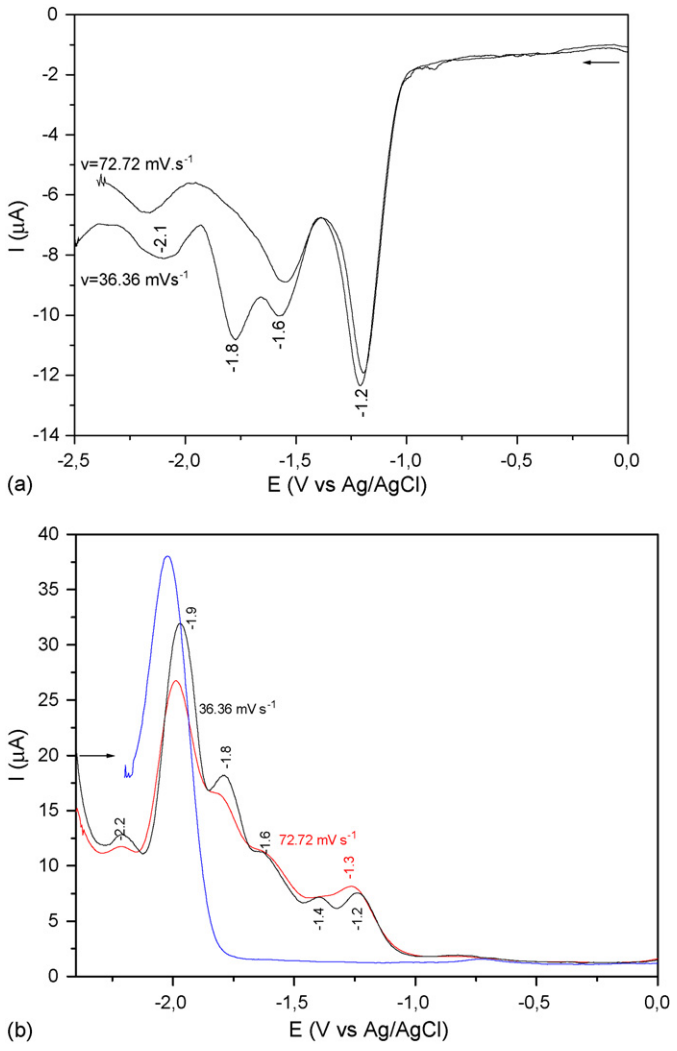

Fig. 6. Differential pulse voltammogram of the $[ZrCl_2(pyrone)_2]$ complex. (a) Cathodic scan; (b) anodic scan (complex and pyrone).

The reduction potential values for $[ZrCl_2(pyrone)_2]$, are more negative than the first and second peaks in the titanium one. This means that the Zr(IV) complex is more stable than the analogous Ti(IV) complex.

The reduction process concerning the Ti(IV) and Zr(IV) complexes can be represented through the set of equations shown in Scheme 3.

The reduction waves at −2.2 and −2.1 V, observed in the cyclic voltammogram of the Ti(IV) and Zr(IV) complexes, should be related to the reduction involving the ligand, since for free ligand there is a reduction process at −2.0 V. The ligand coordination to the metal center provides a peak shift, so that it becomes unfavorable for ligand reduction.

These assignments of the detected waves as the reduction of the ligand or of the metal ion are further supported by controlled potential electrolysis for Ti(IV) and Zr(IV) complexes. In each case, the electronic spectra, as well as current–potential profile, were also registered.

The electronic spectrum of the pyrone ligand shows a band at 272 nm (Fig. 7, curve a). After electrolysis at −2.2 V versus

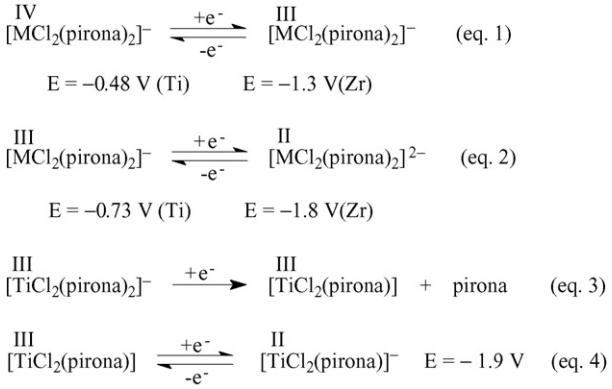

Scheme 3.

Ag/AgCl, there is a color change in the solution, from transparent to yellow and an absorption band is detected at 345 nm (Fig. 7, curve b). The pyrone coordinated to $[ZrCl_2]$, has bands at 314 and 270 nm (Fig. 7, curve c).

The electrolysis with potential applied at −1.4 or −1.9 V for the zirconium complex does not present significant band shifts in the UV–vis spectrum. However, in the last case (−1.9 V), a color change occurred in the solution, from transparent to yellow. One may suppose that there is no zirconium oxidation state change or that oxidation states, which are less than IV in this compound, do not present absorption bands at regions which differ from that of the complex with Zr(IV) or a slow release of the pyrone ligand.

The titanium complex, after electrolysis with applied potential at −0.9 and −2.0 V, exhibited the same spectroscopic behavior as observed in the case of the Zr(IV) complex.

Cyclic voltammograms registered from the electrolyzed samples of the complexes **1** and **2**, assure that the redox process at −0.48, −0.72, −1.52 and −1.9 V with Ti(IV) complex, and −1.3 and −1.8 V with zirconium complex are found to be centred on the metal ion. Cyclic voltammograms of electrolyzed complexes illustrate that peaks which are attributed to the reduc-

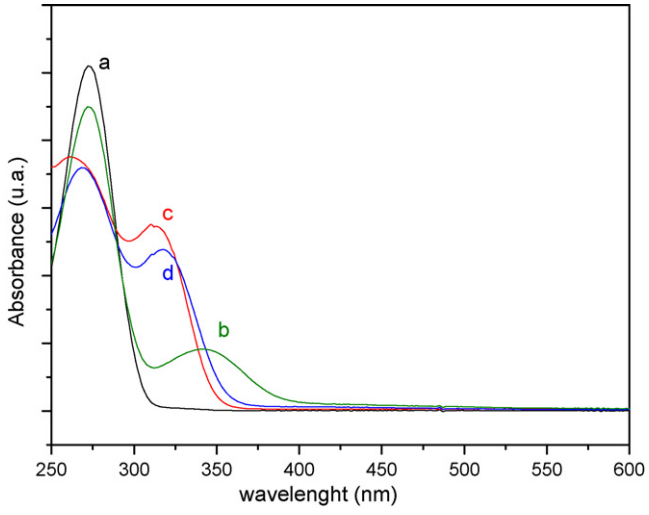

Fig. 7. Electronic spectrum at UV–vis region to the pyrone ligand (a, initial; b, after electroysis) and $[ZrCl_2(pyrone)_2]$ (c, initial; d, after electrolysis).

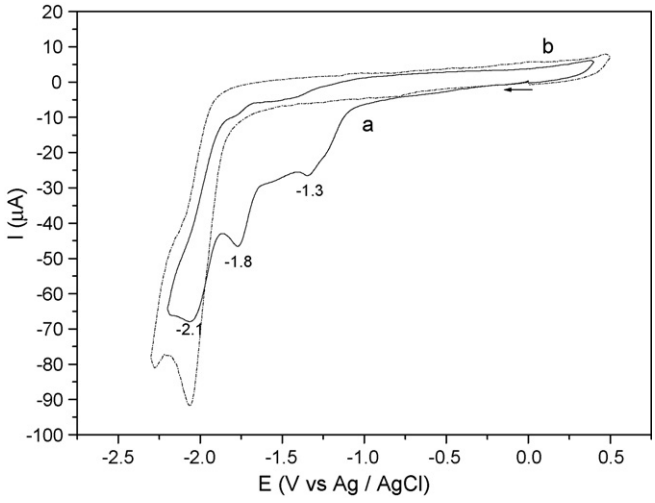

Fig. 8. Cyclic voltammograms of $[ZrCl_2(pyrone)_2]$ complexes. (a) Initial and (b) after electrolysis.

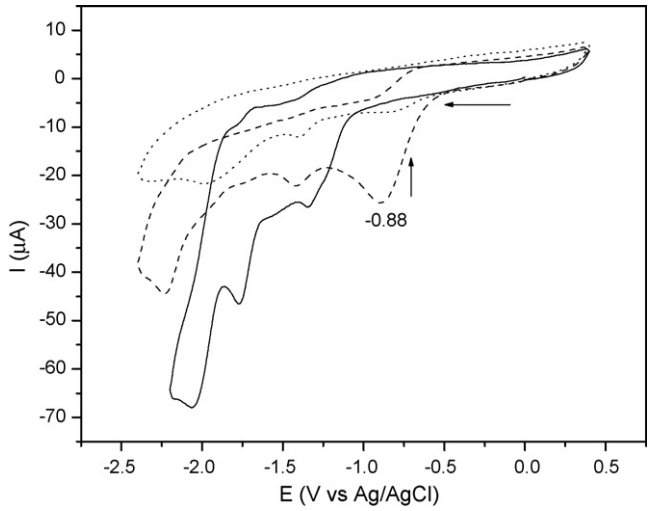

Fig. 9. Sucessive cyclic voltammograms of the $[ZrCl_2(pyrone)_2]$ at Al/Zr = 5 with $v = 200\,mV\,s^{-1}$.

tion process of the metal ions disappear and the profile is similar to that of ligands after electrolysis. This behavior is consistent with ligand release after metal ion reduction (Fig. 8).

In the pyrone ligand voltammogram, before and after electrolysis, applying a potential at −2.2 V, there is a shift in cathodic peak of the voltammogram profile which decreases the cathodic current peak at −2.0 V and shows an anodic peak at +0.2 V.

Table 3 presents the values of the cathodic peaks observed on the electrochemical analysis of the mixture titanium complex with MAO cocatalyst in ethylene atmosphere.

The potential which corresponds to $Ti^{IV/III}$ reduction in the original complex shows a value of −0.48 V. According to Table 3, we observe that in the active species, the displacement is to a more negative potential which reflects a Ti(IV) stabilization. The increase of the Al/Ti ratio and the presence of an ethylene atmosphere do not ilustrate significant variations in the reduction potential values. Therefore, the decrease in catalyst activity observed for such a complex as Al/Ti increases could probably be due the ion pair equilibrium between MAO and cationic species.

The displacement to more negative potentials is not expected during chlorine ligand substitution (electron acceptor) by methyl ligand (electron donor) as occurred in $[TiCl_2(pyrone)]$. The fact is more likely to be related to the cation-methylpyronetitanium species formation that is stabilized by anion $ClMAO^-$, as it was reported in metallocenes [20].

Table 3
Electrochemical data of complex **1** in the presence of MAO and ethylene

Al/Ti	E^{red} (V)	E^{red} (V)/ethylene[a]
1	−1.39; −0.97	−1.41; −0.97
2	−1.41; −0.96	−1.41; −0.96
5	−1.41; −0.63	−1.43; −0.91
10	−1.42; −1.10	nd

nd: not determined.
[a] Ethylene = 1 atm.

The zirconium complex, in the presence of MAO, only shows the stabilization of the active species in the presence of an ethylene atmosphere.

The increase of the Al/Zr ratio does not modify the reducing potential values of the active species. In the presence of MAO, the cyclic voltammogram for $[ZrCl_2(pyrone)_2]$ shows a reduction process at −0.88 V which was absent in the original complex. Considering that: (i) chloro substitution to the methyl group in the analogous titanium complex engenders a displacement of the cathodic potential with more negative potential values, but in this case, an opposite potential shift was observed and (ii) the generated species in the complex mixture with the cocatalyst are only stable under ethylene atmosphere. Thus, it is likely that in this case, there is methyl and ethylene in the coordination sphere of Zr(IV). This behavior can explain the enhancement in catalytic activity as the Al/Zr ratio increases.

The successive cyclic voltammograms for solutions of **1** and **2** complexes with MAO show that the current peaks at −0.48 and −0.88 V decrease with time probably due to the instability of these actives species in solution, as can be seen in Fig. 9.

4. Conclusions

The zirconium complex was shown to be more active in ethylene polymerization (180.0 kg PE/(mol Zr h atm)) than the analogous titanium complex (66.0 kg PE/(mol Ti h atm)). In both cases, catalyst activity was shown to depend on polymerization temperature and on the Al/M ratio. For the zirconium complex, catalyst activity is enhanced as temperature and Al/Zr increase. An opposite trend was observed for the Ti complex. ^1H NMR analyses of the zirconium complex have demonstrated the presence of two main stereoisomers in solution: *cis* and *trans*, as confirmed by the theoretical calculations. The ratio between these two isomers depends on the solvent polarity. The existence of stereoisomers was not observed in the case of the titanium complex.

Taking into account the electrochemical analyses, one may suppose that the better catalytic performance of the zirconium complex is related to the fact that it is more stable in terms of reducing process when compared to the titanium one. Furthermore, cyclic voltammogram illustrated the necessity of the coordination of ethylene in order to stabilize the zirconium active species created by the reaction of [$ZrCl_2$(pyrone)] with MAO.

Acknowledgements

We thank CNPq, CAPES and PRONEX/FAPERGS for financial support.

References

[1] G. Talarico, V. Busico, L. Cavallo, Organometallics 23 (2004) 5989.
[2] C. De Rosa, T. Circelli, F. Auriemma, R.T. Mathers, G.W. Coates, Organometallics 37 (2004) 9034.
[3] S.B. Cortright, J.N. Coalter, M. Pink, J.N. Johnston, Organometallics 23 (2004) 5885.
[4] S.D. Ittel, L.K. Johnson, M. Brookhart, Chem. Rev. 100 (2000) 1169.
[5] M.P. Gil, J.H.Z. Dos Santos, O.L. Casagrande Jr., J. Mol. Catal. A: Chem. 209 (2004) 163.
[6] P. Sobota, Coord. Chem. Rev. 248 (2004) 1047.
[7] P. Sobota, K. Przybylak, J. Utko, L.B. Jerzykiewikz, A.J.L. Pombeiro, M.F.G. da Silva, K. Szczegot, Chem. Eur. J. 7 (2001) 951.
[8] C. Carone, V. de Lima, F. Albuquerque, P. Nunes, C. de Lemos, J.H.Z. dos Santos, G.B. Galland, F.C. Stedile, S. Einloft, N.R. de S. Basso, J. Mol. Cat. A: Chem. 208 (2004) 285.
[9] P. Greco, R. Brambilla, S. Einloft, F.C. Stedile, J.H.Z. dos Santos, G.B. Galland, N.R. de S. Basso, J. Mol. Cat. A: Chem. 240 (2005) 61.
[10] R. Fusco, L. Longo, A. Proto, F. Mais, G. Garbassi, Macromol. Rapid Commun. 19 (1998) 257;
(a) M.J. Frisch, G.W. Trucks, H.B. Schlegel, G.E. Scuseria, M.A. Robb, J.R. Cheeseman, V.G. Zakrzewski, J.A. Montgomery Jr., R.E. Stratmann, J.C. Burant, S. Dapprich, J.M. Millam, A.D. Daniels, K.N. Kudin, M.C. Strain, O. Farkas, J. Tomasi, V. Barone, M. Cossi, R. Cammi, B. Mennucci, C. Pomelli, C. Adamo, S. Clifford, J. Ochterski, G.A. Petersson, P.Y. Ayala, Q. Cui, K. Morokuma, D.K. Malick, A.D. Rabuck, K. Raghavachari, J.B. Foresman, J. Cioslowski, J.V. Ortiz, B.B. Stefanov, G. Liu, A. Liashenko, P. Piskorz, I. Komaromi, R. Gomperts, R.L. Martin, D.J. Fox, T. Keith, M.A. Al-Laham, C.Y. Peng, A. Nanayakkara, C. Gonzalez, M. Challacombe, P.M.W. Gill, B. Johnson, W. Chen, M.W. Wong, J.L. Andres, C. Gonzalez, M. Head-Gordon, E.S. Replogle, J.A. Pople, Gaussian 98, Revision A.5, Gaussian, Inc., Pittsburgh, PA, 1998.
[11] C. Lee, W. Yang, R.G. Parr, Phys. Rev. B 37 (1988) 785.
[12] A.D. Becke, Phys. Rev. A 38 (1988) 3098.
[13] T.H. Dunning Jr., P.J. Hay, in: H.F. Schaefer III (Ed.), Modern Theoretical Chemistry, vol. 3, Plenum Press, New York, 1976, pp. 1–27.
[14] P.J. Hay, W.R. Wadt, J. Chem. Phys. 82 (1985) 270.
[15] W.R. Wadt, P.J. Hay, J. Chem. Phys. 82 (1985) 284.
[16] P.J. Hay, W.R. Wadt, J. Chem. Phys. 82 (1985) 299.
[17] R. Fusco, L. Longo, A. Proto, F. Mais, G. Garbassi, Macromol. Rapid Commun. 19 (1998) 257.
[18] D. Coevoet, H. Cramail, A. Deffieux, Macromol. Chem. Phys. 199 (1998) 1451.
[19] L. Matilainem, M. Klinga, M. Leskelã, J. Chem. Soc. Dalton Trans. (1996) 216.
[20] J. Pédeutour, K. Radhakrishnan, H. Cramail, A. Deffieux, J. Mol. Catal. A: Chem. 185 (2002) 119.